Microbial fuel cells connected in series in a common electrolyte underperform: Understanding why and in what context such a set-up can be applied

Manon Oliot[a,*], Luc Etcheverry[a], Renaut Mosdale[b], Alain Bergel[a]

[a] Laboratoire de Génie Chimique, CNRS, Université de Toulouse (INPT), 4 allée Emile Monso, 31432 Toulouse, France
[b] PaxiTech SAS, 32 rue de Comboire, 38130 Echirolles, France

Keywords:
Numerical modelling
potential distribution
current line
bioelectrochemical system
electromicrobial snorkel

A B S T R A C T

Microbial fuel cells (MFCs) have the outstanding ability to transform the chemical energy contained in organic matter directly to electrical energy. Unfortunately, they give only low cell voltage at maximum power. Connecting several MFCs electrically in series inside the same reactor may be a way to increase the cell voltage, but experimental attempts have shown poor efficiency for such single-electrolyte stacks.

The present study uses numerical modelling to understand the behaviour of single-electrolyte MFC stacks and to assess possible ways to improve it. The numerical model was validated by comparison with two experimental MFCs that produced 0.85 ± 0.05 mW each at 0.23 V cell voltage. Connected in series in a common electrolyte, the stack produced only 0.7 mW at 0.21 V, while, in theory, 1.7 mW could be reached at 0.47 V. The model showed that the drastic power loss was due to ionic short-circuiting, which may, however, be an interesting phenomenon to be exploited for designing an electro-microbial snorkel. The model also showed that decreasing the anode-cathode distance, increasing the distance between the MFCs or using baffles between them could optimize the single-electrolyte stack to produce up to 80% of the theoretical maximum power. Nevertheless, such designs are appropriate only for specific applications, e.g. biosensing. The model further suggests that benthic MFCs could be effectively connected in series.

1. Introduction

Microbial fuel cells (MFCs) have the outstanding capacity to transform the chemical energy contained in low-cost, renewable organic matter directly into electrical energy. Their global performance remains limited; 6.4 $W.m^{-2}$ has recently been claimed to be the highest power density supplied so far by a laboratory prototype [1]. Nevertheless, the low power supplied is not an unsurmountable obstacle for some future applications [2]. Actually, impressive demonstrations of the capacity of MFCs to satisfy the requirements of low-power-consuming devices started to be made more than a decade ago [3]. Various sensors and telecommunication systems have been powered by MFCs [4–6] and, in this framework, sediment MFCs have shown interesting capabilities [7–9]. Fun applications such as feeding a micro-robot with insect material [10] and powering a mobile phone with urine [11,12] have also helped to enlarge the possible application fields. Recently, an MFC designed as a "floating garden" that supplied LED-lights and a data transmission device [13] was presented at the 2015 Universal Exposition. Nevertheless, a few stumbling blocks still have to be overcome before the real potential of the technology can be clearly assessed. A major concern in MFC development is the low cell voltage that is produced when they operate at maximum power [9,14].

The cell voltage of a single MFC unit can be increased by using dedicated electronic harvesting systems [9,15,16] but a part of the power produced by the cell is consumed by the electronic power management system. Another option is to connect several individual MFCs electrically in series. In theory, the voltage provided by the MFC stack is the sum of the voltages of the individual cells but, in practice, tricky control problems arise [17]. As each MFC is allowed to evolve in its own way, the cells can drift to different behaviours, which often results in some MFCs working in electrolysis mode rather than power producing mode

* Corresponding author. Manon Oliot, (+33) 5 34 32 36 28.
E-mail addresses: manon.oliot@ensiacet.fr, manon.oliot@gmail.com (M. Oliot), luc.etcheverry@ensiacet.fr (L. Etcheverry), renaut.mosdale@paxitech.com (R. Mosdale), alain.bergel@ensiacet.fr (A. Bergel).

http://dx.doi.org/10.1016/j.electacta.2017.06.114

Glossary

Parameter

B	distance between the reactor wall and MFCs (cm)
d	anode-cathode distance (cm)
D	distance between MFCs (cm)
e	width between the baffles (cm)
E	Nernst potential (mV)
i_{max}	anodic maximum current (mA)
i_0	cathodic exchange current (mA)
K_M	substrate affinity constant (mol.L^{-1})
K_1, K_1	Kinetic parameters (–)
S	substrate concentration (mol.L^{-1})
U_{cell}	cell voltage (V)
W	reactor depth (cm)
α	charge transfer coefficient (–)
σ	electrolyte ionic conductivity (S.m^{-1})
φ	electrostatic potential (mV)

Subscript

A	Anode
C	Cathode
M	Electrode material
S	Solution

(voltage reversal) [18,19]. In practice, the cell voltage provided by MFC stacks can be much lower than the sum of the voltages of the individual cells. A power management unit must consequently be implemented to avoid voltage reversal and boost the stack towards the theoretical maximum power [20,21].

Immersing all the MFCs that are electrically connected in series in a common reactor may be an interesting way to mitigate the deviations of individual cells, as all the cells would thus be exposed to the same electrolyte under the same conditions. Moreover, a single-electrolyte reactor would allow compact devices to be designed, in which the risk of liquid leaks would be limited, maintenance simplified, and the MFCs supplied with fuel in an easier way than with individual cells. In spite of these obvious advantages, only a few experimental attempts concerning MFC stacks in a single reactor have been reported [22–24], likely because such a design has shown poor efficiency. Connecting several MFC units in series inside the same reactor has resulted in severe voltage loss. The voltage of the stack is generally considerably lower than the sum of the voltages of the individual cells. For example, four MFCs, each ensuring a cell voltage of 0.34 V, resulted in only 0.73 V when connected in series in the same reactor [23]. Similarly, four MFCs, each producing 6.5 W.m^{-3}, resulted in 14.7 W.m^{-3} [24]. The energy loss has been attributed to lateral ion cross-conduction between the cells [24], by analogy with what has been observed in arrays of chemical fuel cells [25]. Increasing the distance between the MFC units has been proposed to mitigate the voltage loss. For instance, when the distance between two MFC units was increased from 1 to 8 cm, the percentage voltage loss decreased from around 46.5% to 44% [22].

An intermediate way has consequently often been used by connecting individual MFCs through a hydraulic network. When the hydraulic connection is in parallel, the different MFCs are supplied with the same electrolyte and, when the hydraulic connection is in series, the different MFCs are supplied with almost the same electrolyte, if depletion of the substrate(s) and accumulation of metabolite(s) are not too important. Even in this case, the voltage of the MFCs connected in series is generally considerably lower than the sum of the voltages of the individual cells [22,26]. Seven miniature MFCs hydraulically linked produced ten times less current when electrically connected in series instead of parallel [27]. As observed with MFC units inside the same reactor, increasing the distance between MFCs has also been reported as a possible solution in this case [28]. The connection of individual MFCs through a hydraulic network was not considered here because the motion of the electrolyte through the different MFC cells consumes a lot of power, which limits the field of possible application types. In this context, the first self-sustained stack, achieved recently, required the connection of 40 MFC units to power the pump and the electronic control device [29]. The present study deals with the electrical connection of MFC units inside the same reactor without a hydraulic network.

As the problem is related to ionic conduction inside the stack, modelling the potential distribution should provide the most appropriate tool to address it in a comprehensive manner. The purpose of this work was to develop MFC numerical modelling to understand the cause of the voltage loss when several MFC units were set inside the same reactor, to determine whether some benefit may be gained, and in what conditions. With this objective, MFCs were designed with an abiotic air-cathode associated with a bioanode formed from compost leachate [30,31]. MFCs were fed with acetate, which was oxidized at the bioanode:

$$CH_3COO^- + 4H_2O \rightarrow 2HCO_3^- + 9H^+ + 8e^- \quad (1)$$

and oxygen was reduced at the cathode:

$$O_2 + 4e^- + 2H_2O \rightarrow 4OH^- \quad (2)$$

A numerical model was developed to map the electrostatic potential distribution inside the cells. The model was first validated by comparison with the experimental data and was then used to predict the performance of a single-electrolyte MFC stack by varying the architecture of the stack. The model allowed different stack architectures and large ranges of parameter values to be explored very fast so as to guide further experimental confirmation with the most appropriate designs and conditions.

2. Experimental

2.1. Microbial anode formation

Microbial anodes were first formed under constant applied potential in 650 mL 3-electrode set-ups. A carbon cloth (PaxiTech SAS, Grenoble, France) of 3×3 cm^2 geometric surface area connected to a platinum wire was used as the anode (working electrode), a platinum grid as the auxiliary electrode and a saturated calomel electrode as the reference (SCE, potential +0.24 V/SHE). A potential of −0.2 V/SCE [30,31] was applied using a VSP potentiostat (Bio-Logic SA, France). Current was recorded as a function of time (chronoamperometry, CA) and successive additions of sodium acetate 20 mM were made when the current fell to around zero. Reactors were kept in a heat chamber at 40 °C, which is the optimal temperature in the range from room temperature to 60 °C [32,33].

A leachate of garden compost was obtained by filtering a mix of 1.5 L of garden compost and 2.25 L of water, containing 60 mM KCl, through a cloth with a large mesh. This leachate served as both the culture medium and the inoculum for the first phase of the bioanode formation. Once oxidation peaks on CA indicated mature bioanodes (current around 15 mA), generally after 3 acetate additions, the compost leachate was replaced by a synthetic medium, which contained 50 mM bicarbonate buffer, 10 mL.L^{-1} macronutrients, 1 mL.L^{-1} micronutrients, 1 mL.L^{-1} vitamins, 4.5 g.L^{-1} KCl and 2.4 g.L^{-1} $NaH_2PO_4.H_2O$. pH was adjusted to 7.0. The aim

of this operation was to operate in a clean medium in order to decrease (bio)fouling of the cathode surface [34].

2.2. MFC operation

Two microbial anodes formed under CA were then transferred into the MFC setup. The reactor, of 1.8 L volume, was equipped with two air-cathodes placed on the same face at a distance D = 8.5 cm apart and the anode-cathode distance, d, was 5 cm (Fig. 1.A). The reactor depth (W) was 7 cm. The air-cathodes (PaxiTech SAS, Grenoble, France) were made with a catalyst ink composed of 40% Pt/C catalyst (Tanaka), 1% PTFE solution, ethanol and water, which was sprayed onto a carbon non-woven gas diffusion layer with a SonoTek coating machine. A stainless steel electrical collector was placed against the side of the air-cathode exposed to air. Each air-cathode was circular and the diameter of the operating area was 4.2 cm (surface area 13.85 cm^2). The electrolyte was the synthetic medium with a 20 mM concentration of acetate, which resulted in a conductivity of 1.2 $S.m^{-1}$. MFCs were kept in a heat chamber at 40 °C.

Power curves were recorded by varying the external resistance from 0 to 33,000 Ω and measuring the voltage using a voltmeter with high entry impedance (Keithley 2000 multimeter, USA). A saturated calomel reference electrode was added to the setup to obtain the anode and cathode potentials during power curve recordings. The ohmic resistances between the anode and the reference electrode and the cathode and the reference electrode were measured by electrochemical impedance spectroscopy (EIS). EIS was performed in potentiostatic mode by applying potential values to the anode and the cathode to obtain currents of 5, 10 and 25 mA, which spanned the range currently produced by the MFCs. Frequency ranged from 100 kHz to 10 mHz with a sinusoidal perturbation amplitude of 10 mV.

The numerical model was solved with the Comsol Multiphysics software equipped with the "Electrochemistry" module (version 5).

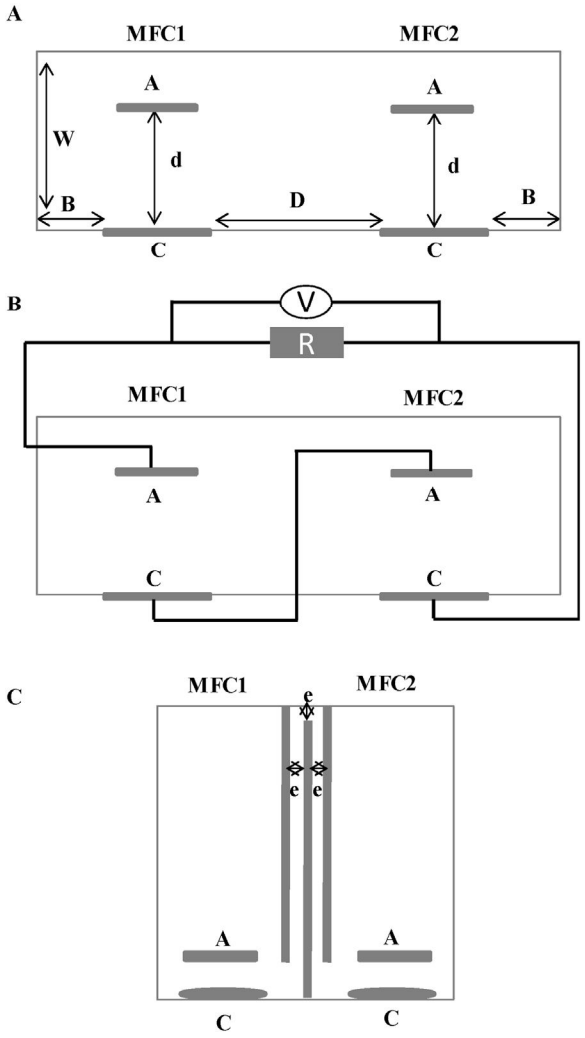

Fig. 1. Scheme of the single-electrolyte MFC stack composed of two MFCs. A: anode. B: distance between the reactor wall and MFCs. C: cathode. d: anode-cathode distance. D: distance between MFCs. e: width between the baffles. W: reactor depth. (A) Experimental device: each MFC has an anode-cathode distance, d, = 5 cm, MFCs are separated by a distance, D, = 8.5 cm. The reactor depth, W, is 7 cm, MFCs are 4 cm away from the reactor wall. (B) Scheme of the series connections of the two MFCs. (C) Optimal device given by the model; MFCs are separated by three baffles that form a path of width e = 5 mm.

3. Results and discussion

3.1. Experimental results

Two bioanodes were formed in parallel in 3-electrode set-ups under constant polarization at −0.2 V/SCE with successive batches of 20 mM acetate and then transferred into the MFC stack, each in front of an air-cathode (Fig. 1.A). Two MFC units (MFC1 and MFC2) were thus designed inside a common electrolyte.

MFC1 and MFC2 were first characterized independently. The power curves (Fig. 2.A and B) showed maximum powers of the same order of magnitude (0.9 and 0.8 mW). Open circuit voltages were 0.67 V and 0.66 V and the cell voltages measured at the maximum power also showed similar values (0.24 and 0.23 V, for MFC1 and MFC2 respectively). Power densities calculated with respect to the anode geometric surface area, of 1 $W.m^{-2}$, were modest compared to the maximum of 7 $W.m^{-2}$ previously obtained with a similar system [35]. Nevertheless, in the previous work, the MFC was designed to maximize the power density by using a cathode with a surface area 19 times larger than that of the anode and a small solution volume of 75 mL. Here, the geometrical parameters were far from the values required to maximize power density. The anode and cathode surface areas were 9 cm^2 and 14 cm^2, respectively, and the solution volume was 1.8 L. It is known that power density decreases dramatically when the electrode areas or the solution volume are increased [36,37]. For instance, it was recently claimed that 2 $W.m^{-2}$ was the highest power density achieved using an air-cathode MFC with a volume greater than 100 mL [38]. The power densities of 1 $W.m^{-2}$ obtained here in cells of 1.8 L volume were consequently consistent with the current performance of the state of the art.

MFC1 and MFC2 were then electrically connected in series. In theory, if two individual cells are connected in series, the same current intensity flows through the two modules and the two cell voltages add up. The theoretical power curve of a stack composed of MFC1 and MFC1 connected as individual cells is obtained by multiplying the values of current intensity by the sum of the MFC1 and MFC2 cell voltages. A maximum theoretical power of 1.7 mW is thus expected, with a theoretical stack voltage of 0.47 V at the maximum power point.

In contrast, the experimental power curve in Fig. 2.C displayed drastically lower performance when MFC1 and MFC2 were connected in series in the same electrolyte. The maximum power measured experimentally was only 0.7 mW and the corresponding stack voltage was 0.21 V. This experiment fully confirmed that connecting two MFCs in series in a common electrolyte results in a considerably lower voltage than the sum of the cell voltages of the

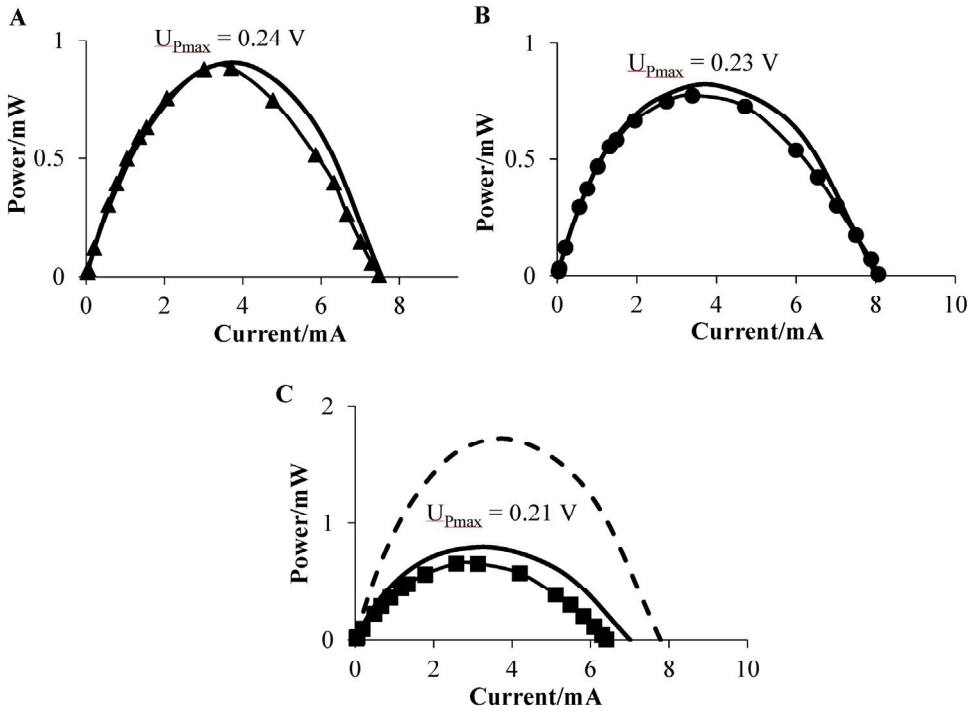

Fig. 2. Experimental (marked line) and modeled (solid line) power curves of (A) single MFC1; (B) single MFC2; (C) MFC1 and MFC2 connected in series in the same electrolyte; The dotted line represents the theoretical curve for two individual MFCs connected in series. According to this curve, MFC1 and MFC2 connected in series as individual cells could theoretically produce a maximum of 1.7 mW under 0.47 V.

individual cells. This was consequently a suitable experimental basis to validate the numerical model.

The whole experimental procedure was reproduced with fresh inoculum. Two other bioanodes were prepared but, in this case, the position of the bioanodes in the stack was changed, each was placed perpendicularly to the air cathode. This configuration led to identical general behaviours, with maximum powers of 0.89 and 0.69 mW for MFC1 and MFC2 respectively, and 0.9 mW for the two MFCs connected in series in the same electrolyte.

3.2. Numerical modelling

3.2.1. Numerical model design

The numerical model was based on the calculation of the secondary potential distribution in the electrolyte by solving the Laplace equation. The electrochemical kinetics of the electrodes were used as the boundary conditions. The theoretical basis and the numerical procedure have already been described in detail for the case of a microbial electrolysis cell [39]. They were similar here for an MFC.

The anodic and cathodic current-potential curves (i-E) were recorded at the same time as the power curves thanks to a reference electrode set in the MFC (Fig. 3). The experimental (i-E) curves were corrected of the ohmic drop by removing the product R.i from each E value, where R is the ohmic resistance between the anode and the reference electrode, or the cathode and the reference electrode. These ionic resistances measured by electrochemical impedance spectroscopy were 4 and 9 Ω, respectively. The higher value of ohmic drop for the cathode was logical because

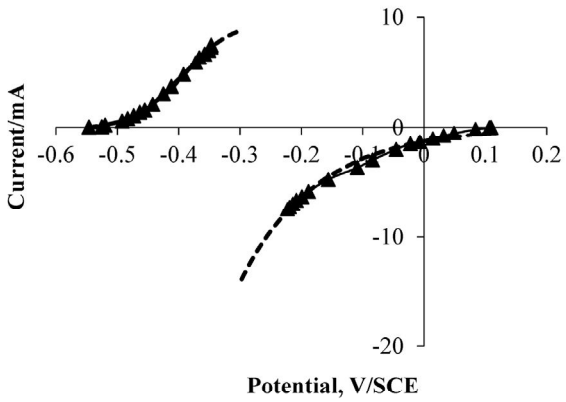

Parameters		
Anode	i_{max}/mA	12
	α_{anode}	0.3
	K_1	70
	K_2	0
	K_M/mol.L^{-1}	0.005
Cathode	i_0/mA	0.55
	$\alpha_{cathode}$	0.8

Fig. 3. Experimental (marked line) anode and cathode kinetics of MFC1 after correction from the ohmic drop and their numerical fittings (dashed line). The table gives the values of the five parameters of the Butler-Volmer-Monod equation (bioanode) and the two parameters of the Butler-Volmer equation (cathode) that are adjusted numerically to fit the bioanode kinetics. In both cases the overpotential was measured from the open circuit potential of the electrode.

the reference electrode was closer to the anode. They were corrected for the ohmic drop.

For the bioanodes, the corrected (i-E) curves were fitted numerically using the Butler-Volmer-Monod equation [40], which expresses the current (i) as a function of the overpotential η as:

$$i = i_{max}\left(\frac{1-\exp(-\frac{n.F}{R.T}.\eta)}{K_1.\exp\left(-\frac{(1-\alpha).n.F}{R.T}.\eta\right)+K_2.\exp(-\frac{n.F}{R.T}.\eta)+\left(\frac{K_M}{S}+1\right)}\right) \quad (3)$$

where i_{max} (mA) is the maximum current, n = 8 is the number of electrons produced per mole of acetate (Equation (1)), F = 96 485C. mol^{-1} is the Faraday constant, R = 8.314 J.mol^{-1}.K^{-1} is the universal gas constant, T = 313 K is the temperature, α is the charge transfer coefficient, S = 0.02 mol.L^{-1} is the substrate concentration, K_M (mol.L^{-1}) is the substrate affinity constant and K_1 and K_2 are dimensionless parameters.

For the abiotic cathodes, the (i-E) experimental curves were fitted with a Butler-Volmer equation, which expressed the current as a function of the overpotential η (the anodic branch was neglected):

$$i = -i_0 exp\left[\frac{-\alpha nF}{RT}\eta\right] \quad (4)$$

where i_0 (mA) is the exchange current and n = 4 is the number of electrons consumed per mole of oxygen (Equation (2)).

After correction of the ohmic drop, the experimental (i-E) curves of the bioanode and the cathode were fitted numerically by a conventional least squares procedure. For the bioanodes, the experimental value of the i_{max} parameter was used and the four parameters α, K_M, K_1 and K_2 were numerically adjusted. For the abiotic cathodes, i_0 and α were the adjustable parameters. In each case it was checked that the numerical curve matched the experimental i-E curve perfectly (Fig. 3).

It is important to mention that parameters were adjusted numerically only to transform the experimental i-E points into equations that could be used by the model. In this context, the objective was not to give a physical meaning to the parameter values in order to model the electrode kinetics, but only to have an accurate mathematical representation of the experimental kinetics. From a purely mathematical standpoint, the experimental kinetics can be fitted by any form of equation: polynomial equations for instance. Nevertheless, our experience has shown that polynomial equations are unsafe because they can give unrealistic values, e.g. oscillating values, when they are used outside the restricted range of numerical fitting. A kinetic law is consequently more appropriate to avoid mathematical unrealistic deviation.

3.2.2. Experimental validation of the numerical model

The numerical model was provided with the geometry of the experimental cell, the numerical form of the bioanode and cathode kinetics, and the value of the ionic conductivity of the electrolyte (1.2 S.m^{-1}). All calculations were performed for an acetate concentration of 20 mM. The model gave the potential and current distributions in the MFC electrolyte. The current was then calculated by integrating the current distribution over the electrode surface. The power curve was plotted by calculating the current for cell voltages ranging from the open circuit voltage to zero. Parameters were adjusted numerically only to transform the experimental kinetics into equations that could be used by the model. Then, no parameter was numerically adjusted during the modelling phase.

The power curves provided by the numerical model for MFC1 and MFC2 (solid lines on Fig. 2.A and B) matched the experimental data well. The calculated maximum powers were 0.88 and 0.82 mW, respectively, for MFC1 alone and MFC2 alone. The corresponding cell voltages were 0.2 V for both MFC1 and MFC2. The consistency of the numerical curves with the experimental data confirmed the validity of the numerical approach.

For MFC1 and MFC2 connected in series in the same electrolyte (solid line on Fig. 2.C), the model displayed a maximum power of 0.79 mW at 0.25 V cell voltage. These values are slightly higher than the experimental measurements. Nevertheless, the slight difference is acceptable, considering that several hours elapsed between the initial recording of the electrode kinetics and the recording of the final power curve of the stack. The bioanode and/or the cathode performance may have decreased during that time, which can explain why the stack performance was slightly lower than predicted using the initial electrode kinetics. In any case, the model confirmed that the stack was extremely far from providing the theoretical performance that would be expected for two individual cells connected in series.

The experimental data resulting from the second experimental run with the bioanodes positioned at right angles to the cathodes confirmed the validity of the model.

3.2.3. Stack of independent MFCs vs. common electrolyte

Fig. 4 compares the distribution of electrostatic potential (φ) and the current lines in the electrolyte of MFC1 and MFC2 when they are electrically connected in series:

- as two individual cells (Fig. 4.A),
- as two cells in a common electrolyte (Fig. 4.B).

In each case, the cathode of MFC1 is electrically connected with the anode of MFC2 and the stack voltage is 0.4 V.

In the configuration of two individual cells (Fig. 4.A), potential and current distributions are similar in both cells. These distributions have the conventional pattern produced by two electrodes face-to-face. The potential distribution is mainly parallel to the electrode surfaces except close to the electrode limits, where edge effects are observed. The current lines, which are perpendicular to the potential lines, show the same symmetrical shape. In each individual cell, the current is carried in the electrolyte bulk by the motion towards the anode of the anions that are produced at the cathode and the motion towards the cathode of the cations that are produced at the anode.

In contrast, in the common electrolyte configuration (Fig. 4.B), potential and current distributions are strongly asymmetrical. The current lines show clear interferences between the MFC1 cathode and the MFC2 bioanode, so intensive ion transport occurs between these two electrodes. A significant proportion of the anions that are produced at the MFC1 cathode move towards the MFC2 anode and a significant proportion of the cations that are produced at the MFC2 anode move towards the MFC1 cathode. This ionic short-circuiting between MFC1 cathode and MFC2 anode does not help to increase the stack voltage between the two electrodes because they are electrically connected. This ionic short-circuiting between MFC1 and MFC2 diverts a part of the ion flux that should ensure the transport of electrical current between the anode and cathode of each MFC to a useless motion between the two electrically connected electrodes. The part of the ion fluxes lost in this short-circuiting does not contribute to power production.

The detail of this explanation can be increased by analysing the values of the electrostatic potential of the electrolyte against the electrode surface for each configuration. Fig. 4.A and 4.B present a scheme of the electrostatic potential distribution with values of potential of the electrolyte in contact with the electrode surface at the middle of each electrode.

The cell voltage U_{cell} produced by two MFCs connected in series is defined as:

$$U_{cell} = \varphi_{MC2} - \varphi_{MA1} \quad (5)$$

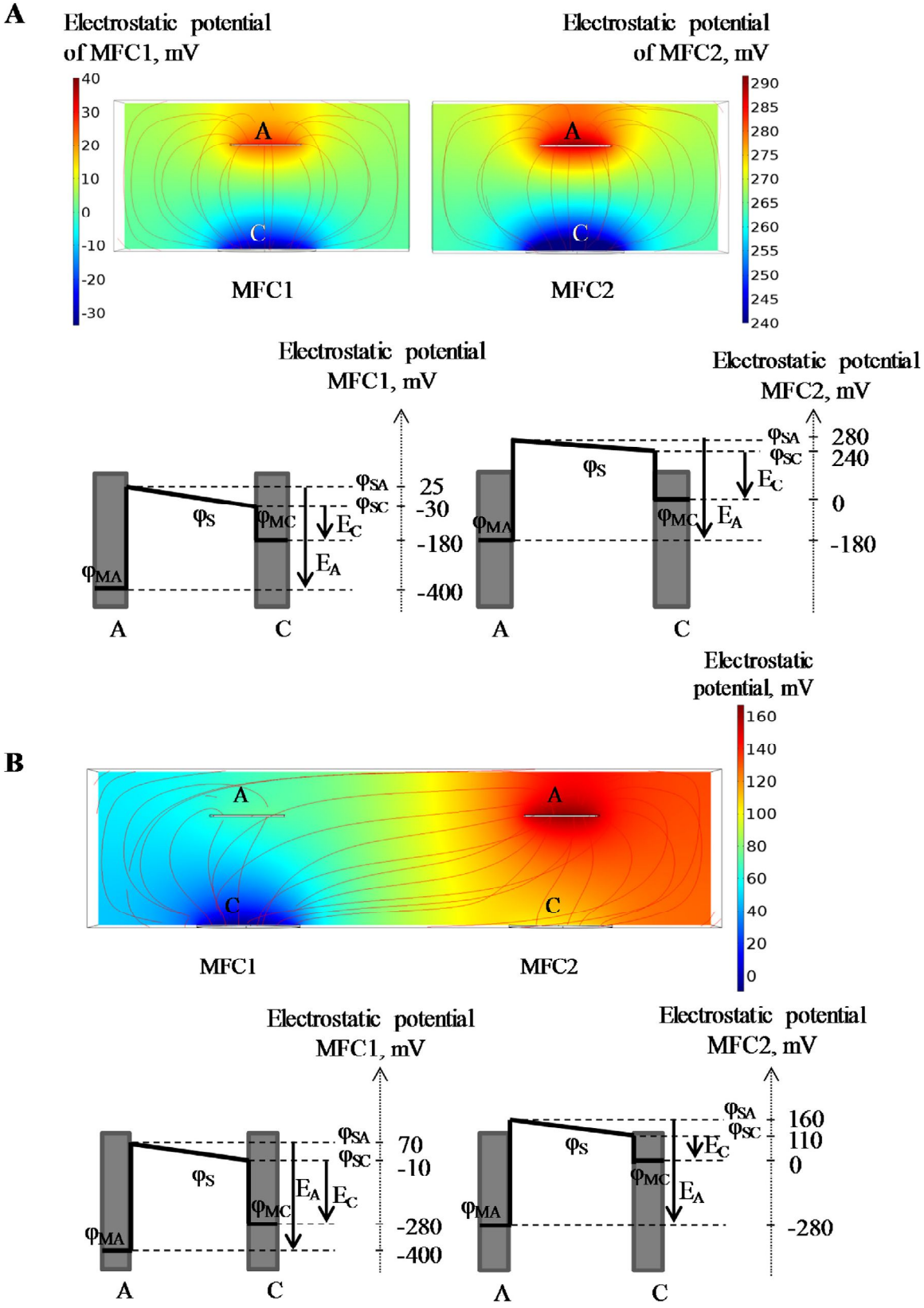

Fig. 4. Potential and current distributions in the electrolyte for a stack voltage of 0.4 V. A) Two individual MFCs connected in series; B) two MFCs connected in series in a common electrolyte. The color scale gives the potential values and current lines are represented in red. U_{cell} 0.4 V, anode-cathode distance 5 cm, MFC distance 8.5 cm, electrolyte conductivity 1.2 $S.m^{-1}$.

where φ_{MC2} and φ_{MA1} are the electrostatic potentials in the electrode material of the MFC2 cathode and the MFC1 anode, respectively. In the present work, the value of the electrostatic potential of the MFC2 cathode material (φ_{MC2}) is arbitrarily chosen as the origin of electrostatic potential and consequently taken to be equal to zero.

The potential/current maps are plotted for the value $U_{cell} = 0.4$ V, so:

$$U_{cell} = -\varphi_{MA1} = 0.4 \text{ V} \quad (6)$$

The values φ_{MA2} and φ_{MC1}, which correspond to the MFC2 anode and MFC1 cathode materials, are extracted from the model and are always equal because the two electrodes are connected electrically.

The Nernst potential of an electrode is defined as the difference between the electrostatic potential of the electrode material (φ_M) and the electrostatic potential of the solution in contact with the electrode surface (φ_S):

$$E = \varphi_M - \varphi_S \quad (7)$$

The Nernst potential of each electrode is calculated by extracting the values φ_{SA1}, φ_{SC1}, φ_{SA2}, φ_{SC2} from the model.

When the two MFCs are connected as individual cells:

- MFC1 Nernst potentials are −0.425 and −0.150 V/SCE at the anode and cathode, respectively,
- for MFC2 Nernst potentials are −0.460 and −0.240 V/SCE at the anode and cathode, respectively.

In this case, obviously, ions cannot move from one cell to the other. Anions produced at a cathode can only migrate to the anode of the same cell, and similarly for cations. All the ions in motion contribute to the transport of electricity from the anode to the cathode inside each MFC.

When the two MFCs are in a single electrolyte, the MFC1 cathode is pushed towards negative Nernst potential (-0.270 V/SCE instead of −0.150 V/SCE with individual cells) while the MFC2 anode is pushed towards higher Nernst potential (-0.440 V/SCE instead of −0.460 V/SCE with individual cells). The MFC1 cathode works at the lowest Nernst potential of the stack and the MFC2 anode works at the highest Nernst potential of the stack, i.e. in the worst conditions for both.

On the other hand, because they are electrically connected, the MFC1 cathode and the MFC2 anode drive intense ion fluxes, which do not help to increase the stack voltage. For example, the anions that are produced at the MFC1 cathode and flow towards the MFC2 anode do not carry current to the MFC1 anode. The MFC1 anode is consequently limited by the low ion transport and is pushed towards low Nernst potential (-0.470 V/SCE instead of −0.425 V/SCE with individual cells). The same situation results in the MFC2 cathode being pushed towards higher Nernst potential (-0.110 V/SCE instead of −0.240 V/SCE with individual cells). The internal current between the MFC1 cathode and the MFC2 anode is consequently high, 7.75 mA, while the electrical current delivered by the stack is only 1.64 mA.

The internal ionic short-circuiting leads the two electrically connected electrodes to overwork, while the anode and cathode connected to the external electrical circuit are underexploited because part of the ion transport is diverted by the ionic short-circuiting.

As a first element of an answer to the title, it can be said that the single-electrolyte configuration leads to ionic short-circuiting between the connected cells, which can result in a drastic loss of power production. Nevertheless, the single-electrolyte configuration boosts the connected anode and cathode to optimal Nernst-potential values; the anode is driven to the highest potential and the cathode to the lowest. This situation results in maximum electric current between the electrically connected electrodes, meaning that they work at high electrochemical reaction rates and consequently consume a large amount of substrate. The single electrolyte configuration can consequently be of interest when the objective is not to produce power but to oxidize substrate, as is the case for effluent treatment, for instance. When the objective is to oxidize the largest possible amount of organic matter, a single-electrolyte stack with MFCs connected in series using a design that ensures strong internal ionic short-circuiting may be an interesting solution. Actually, this design consists in implementing a so-called electrochemical snorkel inside the stack. An electrochemical microbial snorkel consists in short-circuiting an anode with a cathode, so that the current and the rate of consumption of the organic matter are at maximum [41]. This is an extremely simplified system, with low-cost and low maintenance, which should have a promising future in wastewater treatment [42] and environmental depollution [43,44]. Here, a new architecture of electrochemical microbial snorkel is proposed with several short-circuited anode-cathode units. Such a stack provides an easy way of scaling up a snorkel in and, in addition, the last cathode at one end and the last anode at the other give current, which depends directly on the behaviour of the internal electrodes. The internal short-circuited units consume organic matter at the highest possible rate, while the last anode and cathode connected to the external circuit could be used to monitor the process.

3.2.4. Numerical optimization of the single-electrolyte stack configuration

The model was used to assess the extent to which the geometry of the single-electrolyte stack could be improved to obtain performance closer to the theoretical maximum attainable with two MFCs connected as individual cells. The impact of the ionic conductivity of the electrolyte on the optimal stack design was also investigated.

3.2.4.1. Influence of the distance between two MFCs (D). Increasing the distance between the MFC units set inside the same reactor is a way to mitigate the ionic short-circuit in order to enhance the performance of the single-electrolyte stack [22]. The same strategy has been successfully implemented when connecting individual MFC cells through a hydraulic network [28]. Power curves are plotted for increasing values of the distance D between MFC1 and MFC2 in Fig. 5. A distance of 50 cm ensures a significant improvement of the single-electrolyte stack, which thus provides a maximum power of 1.15 mW. Nevertheless, a distance of 3 m is required for the single-electrolyte stack to provide 1.54 mW, i.e. around 90% of the theoretical maximum power (1.7 mW). Moving the two MFCs away from each other clearly mitigates the internal ion short-circuiting. However, in the present case, separating MFC1 and MFC2 by a distance of 3 m would be hardly acceptable from a practical point of view for common laboratory, domestic or industrial applications. This section also illustrates the interest of numerical modelling, which allows a large range of values to be explored and thus takes only a few minutes to give results that would have required a long and cumbersome experimental approach.

3.2.4.2. Influence of the anode-cathode distance (d). Another way to force each MFC to operate more like an individual cell is to reduce the anode-cathode distance. Many recent studies have investigated the so-called Membrane-Electrode Assembly (MEA) configuration, in which a membrane is sandwiched between the anode and the cathode [45,46]. This configuration allows the anode-cathode distance be reduced to a minimum, i.e. to the membrane thickness.

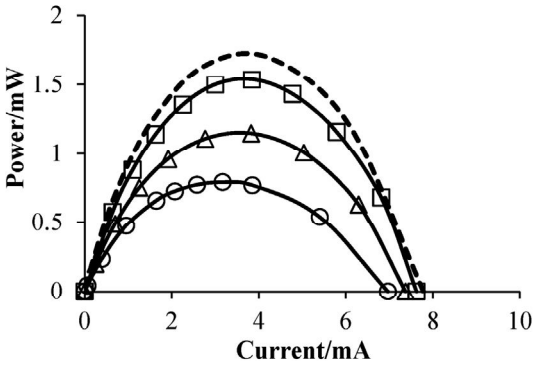

D/cm	Power losses %
8.5	55
50	32
300	9

Fig. 5. Power curves for various distances, D, between two MFCs connected in series in a common electrolyte (marked line, circle: D = 8.5 cm, triangle: D = 50 cm, rectangle: D = 300 cm); anode-cathode distance 5 cm, electrolyte conductivity 1.2 S.m^{-1}. The upper curve (dashed line) corresponds to the theoretical power that should be provided if MFC1 and MFC2 were connected in series as individual cells. The table gives the power loss at the maximum of the power curve vs. the theoretical maximum (1.7 mW under 0.47 V).

The model was run with an anode-cathode distance d = 1 mm, which is representative of an MEA, for comparison with the experimental anode-cathode distance used in this work, d = 5 cm. In this section, the power supply is illustrated in the form of voltage-current (U_{cell}-i) curves (Fig. 6). At any point of the (U_{cell}-i) curve, U_{cell} is higher with the single-electrolyte MEA stack. The model predicts a maximum power of the single-electrolyte stack of 1.33 mW with the MEA (it was 0.79 mW with d = 5 cm) and the maximum stack voltage increases to around 0.35 V (vs. 0.25 V with d = 5 cm). It can be concluded that reducing the anode-cathode distance clearly improves the power and the voltage produced by a single-electrolyte stack.

The theoretical curve that should be obtained with the two MEAs connected as individual cells is also plotted in Fig. 6. It shows that using two MEAs, while keeping the distance between them at 8.5 cm, is not sufficient to push the performance close to the theoretical maximum that could be obtained with individual cells. Reducing the anode-cathode distance has a significant positive impact but is not sufficient to cause the stack to deliver all the power possible.

3.2.4.3. Influence of the electrolyte ionic conductivity. The evolution of the maximum power delivered by the single-electrolyte stack was plotted for three different electrolyte conductivities:

–

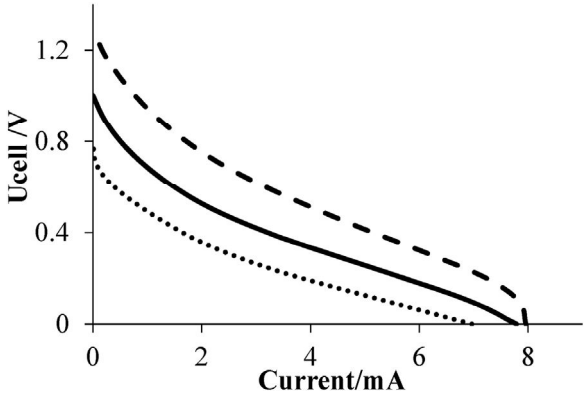

Fig. 6. Cell voltage-current curves of MFC1 and MFC2 connected in series in a common electrolyte (conductivity 1.2 S.m^{-1}) with two different anode-cathode distances, d, of 5 cm (dotted line) or 1 mm (MEA, solid line). The two MFCs are separated by a distance of 8.5 cm. The theoretical curve (dashed line) corresponds to the two MEAs connected as individual cells.

0.5 S.m^{-1}, a value representative of many culture media reported in the literature for MFCs [47,48]
– 1.2 S.m^{-1}, the conductivity of the synthetic medium used in this study
– 5.3 S.m^{-1}, the conductivity of seawater at 25 °C, which is relevant for benthic MFCs

The results are presented in Fig. 7 versus the distance, D, between MFC1 and MFC2.

For a conventional anode-cathode configuration (anode and cathode 5 cm apart, Fig. 7.A), the effect of the ionic conductivity on the single-electrolyte stack is not significant. In any case, MFC1 and MFC2 must be separated by a considerable distance to mitigate ionic short-circuiting. With MFC1 and MFC2 2 m away from each

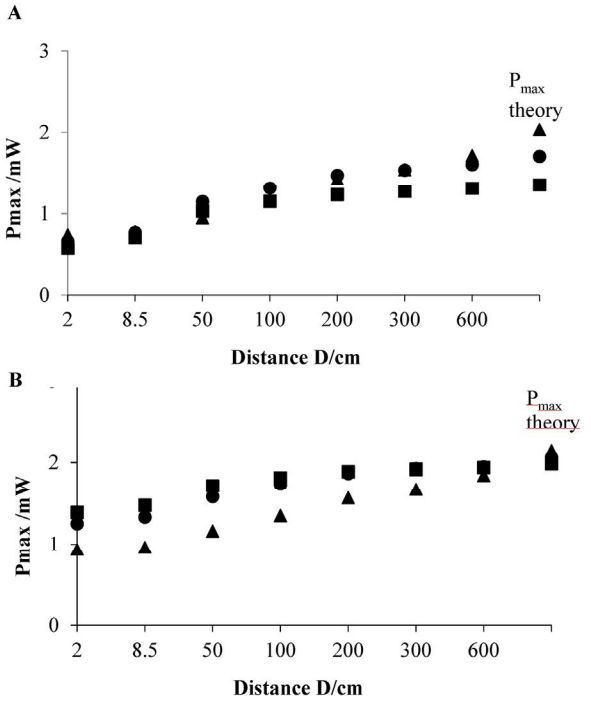

Fig. 7. Maximum delivered power versus the distance between MFC1 and MFC2 in a single-electrolyte stack with an anode-cathode distance d of (A) 5 cm and (B) 1 mm. On each graph, calculations were carried out at three electrolyte conductivities: 0.5 (rectangle), 1.2 (circle) and 5.3 (triangle) S.m^{-1}. The maximum power that could be reached with MFC1 and MFC2 connected as individual cells (or infinite distance in a single-electrolyte stack) is also indicated on each graph.

other, increasing the ionic conductivity by one order of magnitude (from 0.5 to 5.3 $S.m^{-1}$) increases the maximum power only from 1.23 to 1.43 mW (16% increase).

In theory, with individual cells, the same increase in ionic conductivity should increase the power from 1.35 to 2.04 mW (51%). Actually, increasing the ionic conductivity has a beneficial effect as it decreases the internal resistance of each MFC but, in return, it also increases the efficiency of ionic short-circuiting in the single-electrolyte stack. The two phenomena counterbalance each other.

For an MEA (anode and cathode separated by a distance d = 1 mm, Fig. 7.B), the power that would be theoretically supplied by MFC1 and MFC2 connected in series as individual cells does not depend significantly on the conductivity. The theoretical power does not decrease when the conductivity decreases. In an MEA, the ohmic drop is reduced to its minimum because of the small anode-cathode distance, and the influence of ionic conductivity is consequently reduced. MEA confirms that it is an appropriate solution to operate in low conductivity media.

The single-electrolyte stack shows similar behaviour for the two modest conductivities 0.5 and 1.2 $S.m^{-1}$. With MFC1 and MFC2 50 cm apart, around 80% of the theoretical maximum power is achieved, and this percentage reaches 88% when the cells are 1 m apart. The performance falls at the conductivity of seawater (5.3 $S.m^{-1}$). A distance of 6 m between the two cells is required in seawater to obtain 86% (1.84 mW) of the theoretical maximum power (2.14 mW). In MEA configuration, because of the very small anode-cathode distance, the high conductivity of seawater does not have any great beneficial effect on the internal resistance but, in contrast, the high conductivity has a significant detrimental effect by favouring ionic short-circuiting between MFC1 and MFC2.

In conclusion, in a low-conductivity electrolyte, using MEAs connected in series allows the distance between MFC1 and MFC2 to be decreased to 1 m in order to obtain 88% of the theoretical power. For comparison, 3 m distance is required to reach 90% of the theoretical power with a conventional anode-cathode distance of 5 cm. Using MEAs is confirmed to have a clear positive effect by allowing the distance between the two cells to be reduced. Nevertheless, a distance of the order of 50 cm to 1 m remains poorly realistic when the aim is to design a practical stack in laboratory conditions or for portable devices.

In contrast, the model indicates that implementing MFCs connected in series in the sea would be possible, even with a conventional anode-cathode configuration. The distance between MFC1 and MFC2 should be around 6 m, which may be feasible in the sea. Obviously, possible technical constraints, such as power loss due to the Joule effect in the long electrical circuit, remain to be checked.

This preliminary work opens up the interesting possibility that a stack of benthic MFCs connected in series may be a worthwhile solution to increase the power produced, provided that the MFCs are far enough from each other. However, it should be mentioned that the present study was not carried out in the context of benthic MFCs. In particular, the electrochemical kinetics used to validate the numerical model did not correspond to benthic conditions. A dedicated study, which should associate benthic experiments with numerical modelling, will be needed to investigate in depth the research direction, which is suggested here.

3.2.4.4. Geometry optimization. One way to reduce the ionic short-circuiting while keeping a reasonably compact prototype is to place baffles between the two cells. This configuration was modelled with a single baffle or three baffles, which determined a path 5 mm wide (e) and were 5 mm from the reactor wall (Fig. 1.B). MFC1 and MFC2 were assumed to have an anode-cathode distance of 1 mm (MEA) and were 8.5 cm apart in the farthest cases. In this configuration, the theoretical maximum power was 2.08 mW at 0.45 V.

Fig. 8 shows that a single baffle increases the power delivered slightly but the difference is not significant. Three baffles considerably increase the stack performance, with a maximum power of up to 1.92 mW and a stack voltage of 0.4 V. The power curve is close to the theoretical curve that should be obtained if MFC1 and MFC2 were connected as individual cells, showing the maximum theoretical power of 2.08 mW at 0.45 V. A configuration with five baffles does not improve the maximum delivered power significantly (1.97 mW), so the optimum number of baffles can be fixed at three.

The presence of three baffles allows a more compact reactor. Decreasing the distance, D, between MFC1 and MFC2 from 8.5 to 2 cm no longer influences the stack performance. In contrast, the reactor depth does influence the performance. Stack depths of 7, 12 and 20 cm lead to maximum powers of 1.92, 1.98 and 2 mW. This dependence on reactor depth is explained by the elongation of the path imposed on ion motion by the baffles. The greater the depth, the longer the baffle path. Longer baffles efficiently mitigate the ionic short-circuit.

Finally, it was observed that decreasing the distance B between the reactor wall and MFCs from 4 to 1 cm had no influence on delivered power. In conclusion, an efficient stack configuration can be assumed to be composed of two MFCs in MEA configuration (anode-cathode distance 1 mm), 2 cm apart with three baffles in between, and 1 cm from the reactor wall, in a reactor 12 cm deep. With such a configuration, MFCs could be efficiently connected in series in a single electrolyte.

A major advantage of a single-electrolyte stack is to ensure that all MFCs are exposed to the same solution composition. The stack can thus be managed as a single reactor and, in particular, only one inlet is necessary to feed the cell with fuel. In order to check whether this advantage was kept in the presence of baffles, the diffusion rate of acetate along the baffle path was evaluated by the model. The reactor with the geometrical parameters described just above, was taken to be initially fed with a concentration of 50 mM acetate only in MFC1, while the baffle path and MFC2 did not contain any acetate. Ideally, this situation should evolve towards a final uniform concentration of 24 mM in the whole stack at the end of the diffusion process (the MFC1 volume is 720 mL, while the total volume is 1500 mL). The model indicated that, in the absence of stirring, 300 days would be necessary to obtain acetate

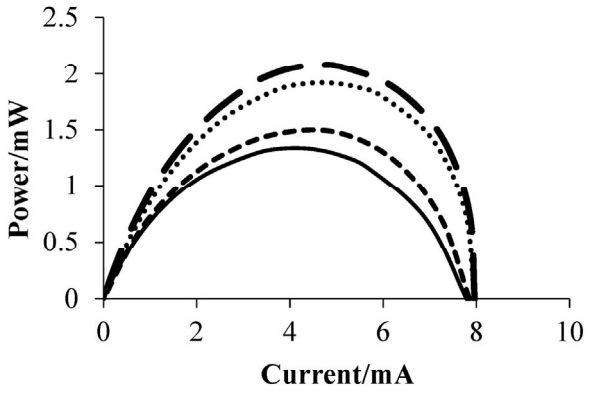

Fig. 8. Power curves without (solid line) and with baffles (big dotted line: single baffle, small dotted line: three baffles) placed between two MFCs connected in series in a common electrolyte; MFCs distance 8.5 cm, anode-cathode distance 1 mm, electrolyte conductivity 1.2 $S.m^{-1}$. The upper curve (dashed line) corresponds to the theoretical power that should be provided if MFC1 and MFC2 were connected in series as individual cells.

concentrations of 1.8 mM in MFC2, while 45.7 mM remained in MFC1 (23.7 mM in the middle of the baffle path). The quantitative value of this result should be qualified because, in reality, the complete absence of any parasite source of stirring (hydrodynamic motion when introducing acetate into the electrolyte, vibrations, temperature gradient, etc.) would be very difficult to achieve. The real diffusion process should consequently be faster than the theoretical rate determined by the model. Nevertheless, the numerical data indicate that diffusion is very slow. In conclusion, the diffusion of the substrate from MFC1 to MFC2 was drastically slowed down by the baffles, and the advantages related to uniform composition inside the stack would be lost.

The presence of a baffled path between the MFCs ensures that all MFCs have the same solution height. In individual MFCS, water evaporation rates may be different from one unit to the other, resulting in MFCs working with different solution levels. Here, this drawback is avoided in the single-electrolyte stack, even when it is equipped with baffles. However, the presence of baffles no longer allows a uniform composition of the electrolyte to be ensured, which makes it necessary to provide an individual substrate inlet for each MFC.

The problem can be solved by using individual MFC cells that are hydraulically connected and forcing the solution to flow along the baffle path, from one MFC to the other. Some large-scale systems have been reported with individual cells connected through a hydraulic network [11] in some cases air gaps were used to isolate different modules that were connected electrically in series [49]. In this case, the pumps needed to achieve the solution flow would consume a lot of power, particularly to move the solution along the long baffle path, or to move the air gaps, probably more energy than the MFC stack can provide in most cases. For instance, the first self-sustained stack, achieved recently, required connecting 40 MFC units to be connected to power the pump and the electronic control device [29]. In the current state of the art, this option is not satisfactory if the main objective is to produce power. Nevertheless, it can have some interest for other applications, for example if a second objective is coupled to power production or is more important than power production, such as sanitation [49] and designing MFC-based biosensors [50]. In this context, a single-electrolyte device equipped with baffles would allow the stack voltage to be increased, thus increasing the sensor sensitivity in terms of biosensing. Increasing the sensitivity of a microbial electrochemical sensor with a single-electrolyte stack could be of great interest, and the pumping energy required would no longer be a decisive criterion.

4. Conclusion

Firstly, numerical modelling shows that strong internal ionic short-circuiting between the anode and the cathode that are electrically connected together is responsible for the drastic loss of power production and cell voltage when MFCs are connected in series in a single electrolyte. However, the electrically connected anode and cathode are pushed to operate at maximum electrochemical rates, which can be of interest when the objective is organic matter abatement for instance.

The model shows that the ionic short-circuiting can be mitigated by distancing MFC1 from MFC2, which allows the theoretical power production to be approached. The model is used to approach an optimal stack configuration by including internal baffles in order to keep the system reasonably compact. This solution diminishes the practical advantages related to uniform concentration inside the stack, but it can be of some interest for specific applications, such as biosensing.

In summary, it can be claimed that connecting MFCs in series in a single electrolyte is possible but requires specific implementation conditions that make the system interesting for specific applications only. In contrast, the model suggests that connecting benthic MFCs in series may be effective. In this context, a dedicated experimental and modelling study is necessary to confirm this interesting possibility.

Acknowledgements

This work benefited from the support of the French state, managed by the Agence Nationale de la Recherche (ANR), within the framework of the Bioelec project (ANR-13-BIME-006). The MFC prototypes were built by the LGC workshop under the guidance of Alain Müller and Vincent Loisel. The authors thank one of the reviewers in particular for careful reading and providing numerous references about actual applications of MFCs.

References

[1] M. Oliot, L. Etcheverry, A. Mosdale, R. Basseguy, M.-L. Délia, A. Bergel, Separator electrode assembly (SEA) with 3-dimensional bioanode and removable air-cathode boosts microbial fuel cell performance, J. Power Sources (2017), doi: http://dx.doi.org/10.1016/j.jpowsour.2017.03.016.
[2] S. Shleev, A. Bergel, L. Gorton, Biological fuel cells: Divergence of opinion, Bioelectrochemistry 106 (2015) 1–2.
[3] A. Shantaram, H. Beyenal, R.R.A. Veluchamy, Z. Lewandowski, Wireless Sensors Powered by Microbial Fuel Cells, Environ. Sci. Technol. 39 (2005) 5037–5042.
[4] A. Dewan, C. Donovan, D. Heo, H. Beyenal, Evaluating the performance of microbial fuel cells powering electronic devices, J. Power Sources 195 (2010) 90–96.
[5] J. Winfield, L.D. Chambers, A. Stinchcombe, J. Rossiter, I. Ieropoulos, The power of glove: Soft microbial fuel cell for low-power electronics, J. Power Sources 249 (2014) 327–332.
[6] F. Khaled, O. Ondel, B. Allard, Microbial fuel cells as power supply of a low-power temperature sensor, J. Power Sources 306 (2016) 354–360.
[7] L.M. Tender, et al., The first demonstration of a microbial fuel cell as a viable power supply: Powering a meteorological buoy, J. Power Sources 179 (2008) 571–575.
[8] C. Donovan, A. Dewan, D. Heo, H. Beyenal, Batteryless, Wireless Sensor Powered by a Sediment Microbial Fuel Cell, Environ. Sci. Technol. 42 (2008) 8591–8596.
[9] Y.R.J. Thomas, M. Picot, A. Carer, O. Berder, O. Sentieys, F. Barriere, A single sediment-microbial fuel cell powering a wireless telecommunication system, J. Power Sources 241 (2013) 703–708.
[10] C. Melhuish, I. Ieropoulos, J. Greenman, I. Horsfield, Energetically autonomous robots: Food for thought, Auton. Robots 21 (2006) 187–198.
[11] I.A. Ieropoulos, P. Ledezma, A. Stinchcombe, G. Papaharalabos, C. Melhuish, J. Greenman, Waste to real energy: the first MFC powered mobile phone, Phys. Chem. Chem. Phys. 15 (2013) 15312–15316.
[12] X.A. Walter, A. Stinchcombe, J. Greenman, I. Ieropoulos, Urine transduction to usable energy: A modular MFC approach for smartphone and remote system charging, Appl. Energy 192 (2017) 575–581.
[13] A. Schievano, et al., Floating microbial fuel cells as energy harvesters for signal transmission from natural water bodies, J. Power Sources 340 (2017) 80–88.
[14] B.E. Logan, M.J. Wallack, K.-Y. Kim, W. He, Y. Feng, P.E. Saikaly, Assessment of Microbial Fuel Cell Configurations and Power Densities, Environ. Sci. Technol. Lett. 2 (2015) 206–214.
[15] H. Wang, J.-D. Park, Z.J. Ren, Practical Energy Harvesting for Microbial Fuel Cells: A Review, Environ. Sci. Technol. 49 (2015) 3267–3277.
[16] X. Zhang, H. Ren, S. Pyo, J.-I. Lee, J. Kim, J. Chae, A High-Efficiency DC-DC Boost Converter for a Miniaturized Microbial Fuel Cell, Ieee Trans. Power Electron. 30 (2015) 2041–2049.
[17] P. Aelterman, K. Rabaey, H.T. Pham, N. Boon, W. Verstraete, Continuous electricity generation at high voltages and currents using stacked microbial fuel cells, Environ. Sci. Technol. 40 (2006) 3388–3394.
[18] J. An, B. Kim, I.S. Chang, H.-S. Lee, Shift of voltage reversal in stacked microbial fuel cells, J. Power Sources 278 (2015) 534–539.
[19] J. An, H.-S. Lee, Occurrence and Implications of Voltage Reversal in Stacked Microbial Fuel Cells, Chemsuschem 7 (2014) 1689–1695.
[20] P. Salvin, O. Ondel, C. Roos, F. Robert, Energy harvest with mangrove benthic microbial fuel cells, Int. J. Energy Res. 39 (2015) 543–556.
[21] F. Khaled, O. Ondel, B. Allard, Optimal Energy Harvesting From Serially Connected Microbial Fuel Cells, Ieee Trans. Ind. Electron. 62 (2015) 3508–3515.
[22] D. Kim, J. An, B. Kim, J.K. Jang, B.H. Kim, I.S. Chang, Scaling-Up Microbial Fuel Cells: Configuration and Potential Drop Phenomenon at Series Connection of Unit Cells in Shared Anolyte, Chemsuschem 5 (2012) 1086–1091.
[23] B. Kim, et al., Voltage increase of microbial fuel cells with multiple membrane electrode assemblies by in series connection, Electrochem. Commun. 28 (2013) 131–134.

[24] B. Wang, J.-I. Han, A single chamber stackable microbial fuel cell with air cathode, Biotechnol. Lett. 31 (2009) 387–393.
[25] R. O'Hayre, T. Fabian, S.J. Lee, F.B. Prinz, Lateral ionic conduction in planar array fuel cells, J. Electrochem. Soc. 150 (2003) A430–A438.
[26] L. Zhuang, S. Zhou, Substrate cross-conduction effect on the performance of serially connected microbial fuel cell stack, Electrochem. Commun. 11 (2009) 937–940.
[27] J. Winfield, I. Ieropoulos, J. Greenman, Investigating a cascade of seven hydraulically connected microbial fuel cells, Bioresour. Technol. 110 (2012) 245–250.
[28] J. Winfield, I. Ieropoulos, J. Greenman, J. Dennis, Investigating the effects of fluidic connection between microbial fuel cells, Bioprocess Biosyst. Eng. 34 (2011) 477–484.
[29] P. Ledezma, A. Stinchcombe, J. Greenman, I. Ieropoulos, The first self-sustainable microbial fuel cell stack, Phys. Chem. Chem. Phys. 15 (2013) 2278–2281.
[30] B. Cercado, et al., Garden compost inoculum leads to microbial bioanodes with potential-independent characteristics, Bioresour. Technol. 134 (2013) 276–284.
[31] S. Parot, M.-L. Delia, A. Bergel, Forming electrochemically active biofilms from garden compost under chronoamperometry, Bioresour. Technol. 99 (2008) 4809–4816.
[32] B. Cercado-Quezada, M.-L. Delia, A. Bergel, Treatment of dairy wastes with a microbial anode formed from garden compost, J. Appl. Electrochem. 40 (2010) 225–232.
[33] B. Cercado-Quezada, M.-L. Délia, A. Bergel, Electrochemical micro-structuring of graphite felt electrodes for accelerated formation of electroactive biofilms on microbial anodes, Electrochem. Commun. 13 (2011) 440–443.
[34] M. Oliot, L. Etcheverry, A. Bergel, Removable air-cathode to overcome cathode biofouling in microbial fuel cells, Bioresour. Technol. 221 (2016) 691–696.
[35] D. Pocaznoi, B. Erable, L. Etcheverry, M.-L. Delia, A. Bergel, Towards an engineering-oriented strategy for building microbial anodes for microbial fuel cells, Phys. Chem. Chem. Phys. 14 (2012) 13332–13343.
[36] I.A. Ieropoulos, J. Greenman, C. Melhuish, Miniature microbial fuel cells and stacks for urine utilisation, Int. J. Hydrog. Energy 38 (2013) 492–496.
[37] I. Ieropoulos, J. Greenman, C. Melhuish, Microbial fuel cells based on carbon veil electrodes: Stack configuration and scalability, Int. J. Energy Res. 32 (2008) 1228–1240.
[38] C. Santoro, S. Babanova, P. Atanassov, B. Li, I. Ieropoulos, P. Cristiani, High Power Generation by a Membraneless Single Chamber Microbial Fuel Cell (SCMFC) Using Enzymatic Bilirubin Oxidase (BOx) Air-Breathing Cathode, J. Electrochem. Soc. 160 (2013) H720–H726.
[39] R. Lacroix, S. Da Silva, M.V. Gaig, R. Rousseau, M.-L. Delia, A. Bergel, Modelling potential/current distribution in microbial electrochemical systems shows how the optimal bioanode architecture depends on electrolyte conductivity, Phys. Chem. Chem. Phys. 16 (2014) 22892–22902.
[40] H.V.M. Hamelers, A. ter Heijne, N. Stein R. A. Rozendal, and C. J. N. Buisman, Butler-Volmer-Monod model for describing bio-anode polarization curves, Bioresour. Technol. 102 (2011) 381–387.
[41] B. Erable, L. Etcheverry, A. Bergel, From microbial fuel cell (MFC) to microbial electrochemical snorkel (MES): maximizing chemical oxygen demand (COD) removal from wastewater, Biofouling 27 (2011) 319–326.
[42] Q. Yang, H. Zhao, H. Liang, Denitrification of overlying water by microbial electrochemical snorkel, Bioresour. Technol. 197 (2015) 512–514.
[43] D.R. Lovley, Live wires: direct extracellular electron exchange for bioenergy and the bioremediation of energy-related contamination, Energy Environ. Sci. 4 (2011) 4896–4906.
[44] C.C. Viggi, et al., The 'Oil-Spill Snorkel': an innovative bioelectrochemical approach to accelerate hydrocarbons biodegradation in marine sediments, Front. Microbiol. 6 (2015) 881.
[45] J.M. Moon, S. Kondaveeti, T.H. Lee, Y.C. Song, B. Min, Minimum interspatial electrode spacing to optimize air-cathode microbial fuel cell operation with a membrane electrode assembly, Bioelectrochemistry 106 (2015) 263–267.
[46] W.-W. Li, G.-P. Sheng, X.-W. Liu, H.-Q. Yu, Recent advances in the separators for microbial fuel cells, Bioresour. Technol. 102 (2011) 244–252.
[47] D. Aaron, C. Tsouris, C.Y. Hamilton, A.P. Borole, Assessment of the effects of flow rate and ionic strength on the performance of an air-cathode microbial fuel cell using electrochemical impedance spectroscopy, Energies 3 (2010) 592–606.
[48] Y. Feng, X. Wang, B.E. Logan, H. Lee, Brewery wastewater treatment using air-cathode microbial fuel cells, Appl. Microbiol. Biotechnol. 78 (2008) 873–880.
[49] I.A. Ieropoulos, et al., Pee power urinal −microbial fuel cell technology field trials in the context of sanitation, Environ. Sci. Water Res. Technol. 2 (2016) 336–343.
[50] D. Davila, J.P. Esquivel, N. Sabate, J. Mas, Silicon-based microfabricated microbial fuel cell toxicity sensor, Biosens. Bioelectron. 26 (2011) 2426–2430.